Optical, thermal and electrical properties of pure and doped bis-thiourea cadmium formate (BTCF) crystal

2014 Phys. Scr. 89 125804

(http://iopscience.iop.org/1402-4896/89/12/125804)

IOP Publishing | Royal Swedish Academy of Sciences Physica Scripta

Phys. Scr. **89** (2014) 125804 (7pp) doi:10.1088/0031-8949/89/12/125804

Optical, thermal and electrical properties of pure and doped bis-thiourea cadmium formate (BTCF) crystal

N N Shejwal[2,3], Mohd Anis[1,3], S S Hussaini[1,3] and M D Shirsat[2]

[1] Crystal Growth Laboratory, Department of Physics, Milliya Arts, Science & Management Science College, Beed-431122, Maharashtra, India
[2] Intelligent Materials Research Laboratory, Department of Physics, Dr Babasaheb Ambedkar Marathwada University, Aurangabad-431004, Maharashtra, India

E-mail: shuakionline@yahoo.co.in

Received 29 April 2014, revised 20 September 2014
Accepted for publication 23 September 2014
Published 24 November 2014

Abstract

A glycine doped bis-thiourea cadmium formate (BTCF) crystal has been grown by a slow solution evaporation technique. The shifts in vibrational frequencies of different functional groups of BTCF were identified by Fourier transform infrared (FT-IR) spectral analysis. UV-visible studies were employed to assess the optical transparency of pure and doped BTCF crystals. The optical band gap of doped BTCF is found to be 5.16 eV. The optical constants, refractive index, reflectance, and optical conductivity have been evaluated, using the transmission data. The dielectric characteristics of pure and doped BTCF were investigated by employing dielectric studies. The decomposition temperature of pure and doped BTCF crystals was determined by using thermogravimetric analysis. The encouraging third-order nonlinear optical properties of pure and doped BTCF crystals were examined by employing the Z-scan technique at 632.8 nm.

Keywords: crystal growth, nonlinear optical properties, electrical properties, thermal properties

1. Introduction

The impressive physico-chemical properties of semiorganic nonlinear materials have drawn the attention of many researchers due to their wide range of applications in laser systems, laser alignment, microelectronics, second harmonic generation (SHG), image processing, data storage, fiber optic communication, optical switching, photonics, and electro-optic modulations [1–4]. The frontier research has been focused on the growth of organometallic compounds, as they offer high stability, large nonlinearity, low angular sensitivity, and good mechanical hardness [5, 6]. In past decade many potential thiourea metal complexes have been reported [5–10]. Bis-thiourea cadmium formate (BTCF) is a promising semi-organic nonlinear optical (NLO) crystal whose morphological, UV-visible, microhardness, thermal, and dc conductivity properties were studied by Selvakumar *et al* and Ravi Kumar *et al* [4, 11].

[3] These authors contributed equally.

In the literature, glycine has been used as a dopant to evaluate the structural, optical, and thermal properties of zinc thiourea sulphate (ZTS) and bis-thiourea cadmium chloride (BTCC) crystals [12, 13]. Hussaini *et al* investigated the effect of glycine on structural, optical, thermal, and SHG efficiency of bis-thiourea zinc chloride (BTZC) crystals [14]. As yet, no systematic third-order nonlinear optical studies of pure BTCF have been conducted; additionally, the effect of glycine on optical, electrical, linear, and nonlinear optical properties remains to be investigated. This paper aims to report the influence of glycine on UV-visible, dielectric, thermal, and third-order nonlinear optical properties of BTCF to explore its effective optical device applicability.

2. Experimental procedure

Analytical reagent (AR) grade cadmium oxide, thiourea, and formic acid were taken in stoichiometric ratio 1:2:2 in

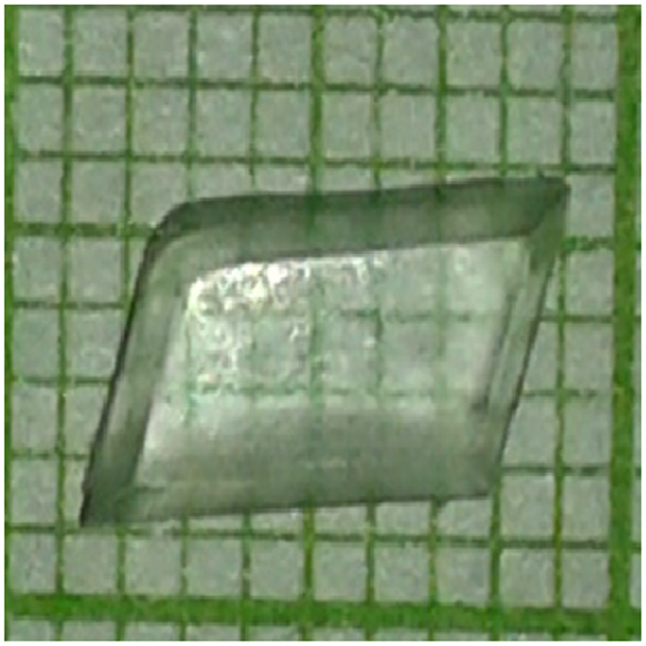

Figure 1. Photograph of glycine doped BTCF crystal.

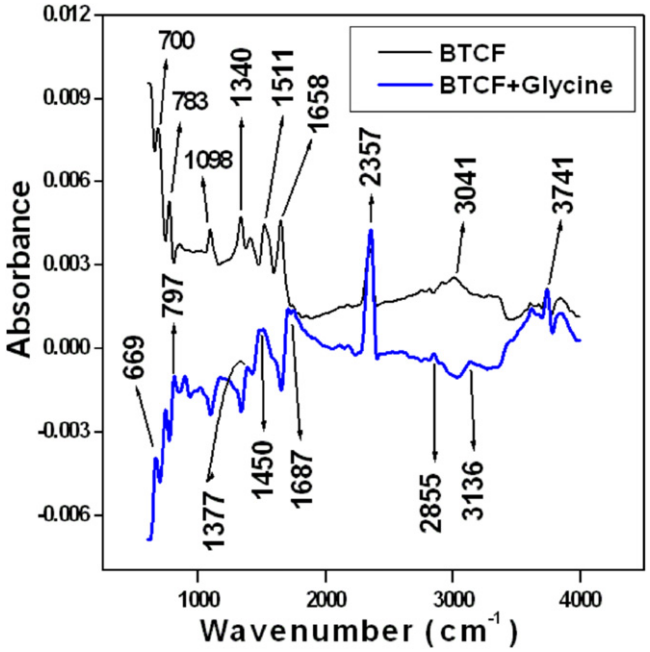

Figure 2. FT-IR spectrum.

deionized water to synthesize BTCF salt. The impurities in BTCF were removed by successive recrystallization. The BTCF was doped with different mole% of glycine to find the most favorable concentration of glycine for our present studies. The calculated amount of 2 mole% glycine was added gradually to the supersaturated solution of BTCF. The solution was stirred at a constant speed for 6 h to achieve the homogeneous doping of glycine in the aqueous volume of BTCF. This solution was filtered and kept for evaporation to obtain the defectless crystal. The synthesized salt was successively recrystallized to achieve high purity. The photograph of glycine doped BTCF crystals obtained in 25 days is shown in figure 1.

3. Results and discussion

3.1. Fourier transform infrared (FT-IR) spectral analysis

The FT-IR vibrational spectra of pure and glycine doped BTCF was recorded, using a Bruker α-ATR instrument in the range 600 cm^{-1}–4000 cm^{-1}, as shown in figure 2. The thiourea ligand formation with cadmium is confirmed by characteristic peaks of BTCF observed at 783, 1098, 1340, 1511, 1658, and 3041 cm^{-1}, which are in good agreement with the reported work [4]. The $-NH_2$ bond stretching is indicated by the absorption peak at 3136 cm^{-1}. The absorption peak at 2855 cm^{-1} occurs due to characteristic C-H stretching of the carbonyl substituent. The bending vibration of the C-H bond is observed at 2357 cm^{-1}. The absorption observed at 1687 cm^{-1} corresponds to C-O-C stretching vibrations. The symmetric N-C-N stretching vibration appears at 1450 cm^{-1}. The peak observed at wavenumber 1377 cm^{-1} is due to C=S stretching vibrations. The absorption peak observed at 797 cm^{-1} is evident of asymmetric O-C-O bond stretching. The peak at 669 cm^{-1} is assigned to N-H bond wagging. The shift in the vibrational frequencies of BTCF, discussed in table 1, indicates the incorporation of glycine in BTCF.

Table 1. Vibrational assignments of pure and glycine doped BTCF.

Wavenumber (cm^{-1})		
BTCF	glycine doped BTCF	Assignments
669	700	N-H wagging
783	797	O-C-O stretching
1340	1377	C=S stretching
1511	1450	N-C-N stretching
1658	1687	C-O-C stretching
	2855	C-H stretching
3041	3136	NH_2 stretching

3.2. Thermogravimetric analysis (TGA)

The thermal decomposition of pure and doped BTCF has been investigated, using the Perkin Elmer thermal analyzer. The TGA analysis was carried out from room temperature to 400 °C in a nitrogen atmosphere at a heating rate of 25 °C min^{-1}. The TGA curves of studied crystals are shown in figure 3. The temperature analysis is vital to understand the extent of materials suitability for optical systems operating at high temperature. The TGA trace of BTCF shows prominent decomposition at 193 °C, which is in good agreement with the reported work [11]. The glycine doped BTCF initiates to decompose at 185 °C, a slightly lower temperature than pure BTCF, which might be due to the unstable nature of amino acids at higher temperatures [14]. Until 185 °C no phase change occurs, and the doped BTCF crystal remains stable, showing its promising quality for device fabrication.

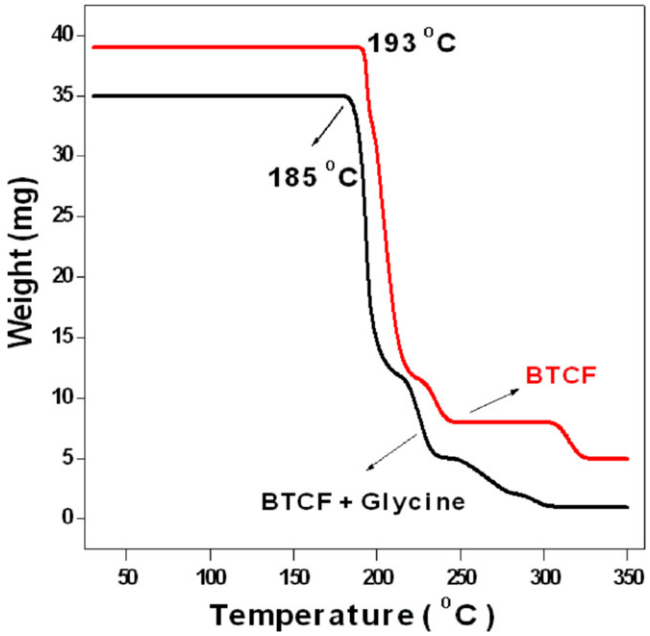

Figure 3. Thermogravimetric curve.

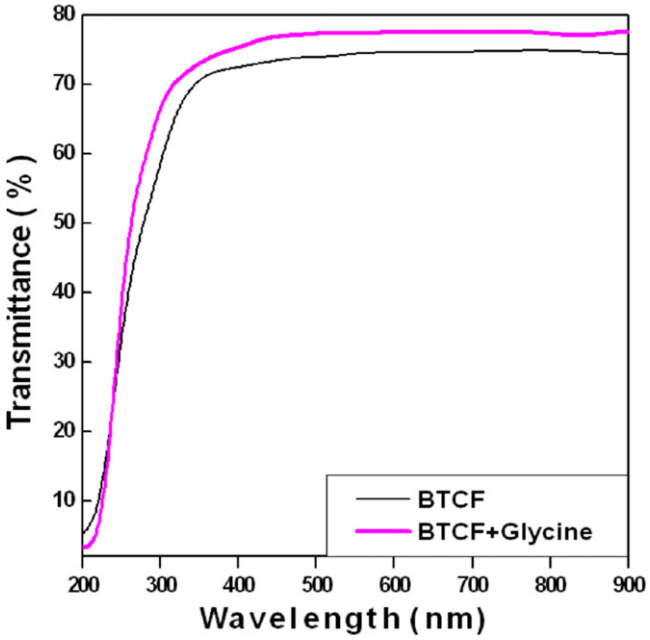

Figure 4. Transmittance spectrum.

3.3. UV-visible studies

The UV-visible studies of pure and glycine doped BTCF crystals were carried out in the range of 200–900 nm, using a Shimadzu UV-2450 spectrophotometer. The transmission study helps to analyze the promotion of electrons to different energy states due to absorption of UV and visible light. The recorded transmission spectrum of pure and glycine doped BTCF crystals is depicted in figure 4. The doped BTCF crystal shows high transmittance and a lower cut-off wavelength (245 nm) than the pure BTCF crystal. The high transparency window and lower cut-off wavelength of the doped BTCF crystal indicates its suitability for SHG device applications [15]. The optical absorption coefficient (α) is determined using the equation $\alpha = 2.303$ log (1/T)/t [16]. The optical band gap (E_g) was evaluated from the equation given as follows [16],

$$(\alpha h\nu)^2 = A\left(h\nu - E_g\right), \tag{1}$$

where A is a constant, E_g is the optical band gap, and hν is the incident photon energy. The optical band gap of pure and doped BTCF crystals was determined using the Tauc's extrapolation plot depicted in figures 5(a) and (b), respectively. The optical band gap of pure BTCF is 5 eV, which is notably greater than the reported value [11]. The optical band gap of doped BTCF is found to be 5.16 eV. The material with a wide optical band gap indicates its suitability for UV tunable lasers and optoelectronics applications [17, 18]. The refractive index (figure 6) and reflectance (figure 7) were calculated using the fundamental equations [16]. The variation of extinction coefficient (K) helps to evaluate the loss of electromagnetic energy within the material medium. The extinction coefficient was evaluated using the relation $K = \lambda\alpha/2\pi$ [16], shown in figure 8. The high transmittance, low refractive index (n), and reflectance (R) of the doped BTCF

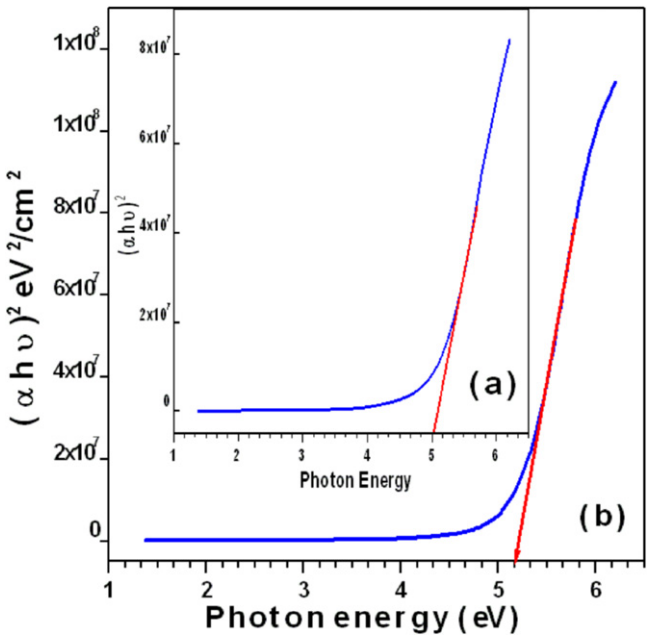

Figure 5. Tauc's plot of (a) BTCF, (b) doped BTCF.

crystal suggest its suitability as an antireflecting transparent window coating material for solar thermal devices [19]. The variation of optical conductivity (σ_{op}) with photon energy is shown in figure 9, which was calculated using the relation as follows,

$$\sigma_{op} = \frac{\alpha n C}{4\pi}, \tag{2}$$

where n is the refractive index and C is the velocity of light. The doped BTCF exhibits a lower extinction coefficient (10^{-5}) and higher optical conductivity ($10^{12}\,s^{-1}$) than pure BTCF, which makes it an efficient material for high speed

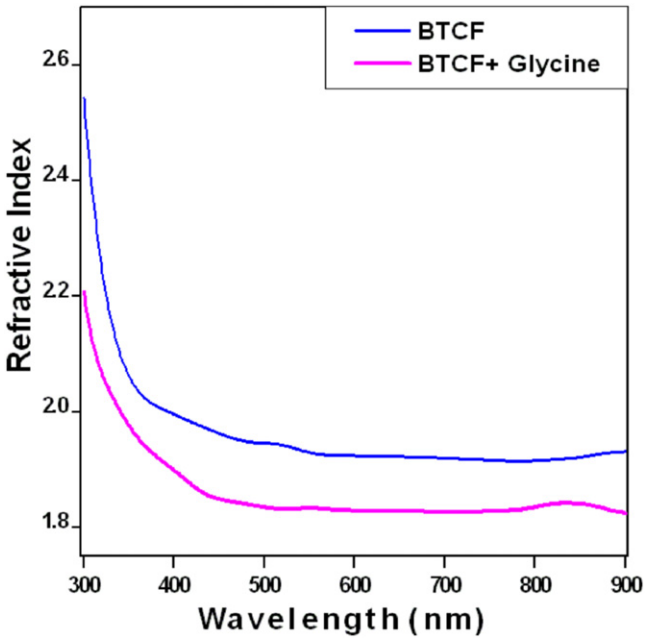

Figure 6. Plot of refractive index as a function of wavelength.

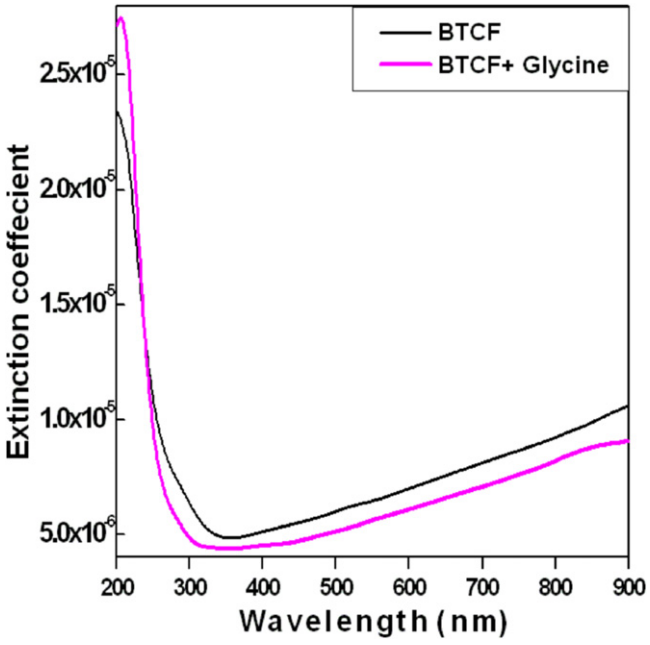

Figure 8. Plot of extinction coefficient as a function of wavelength.

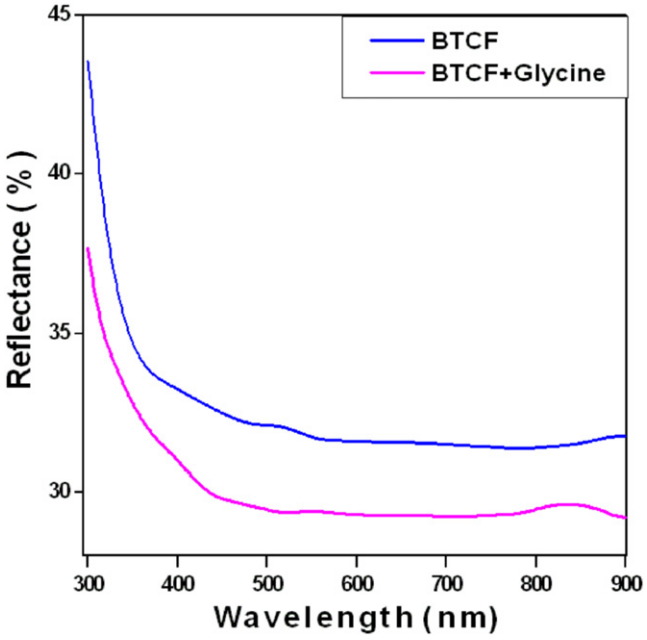

Figure 7. Plot of reflectance as a function of wavelength.

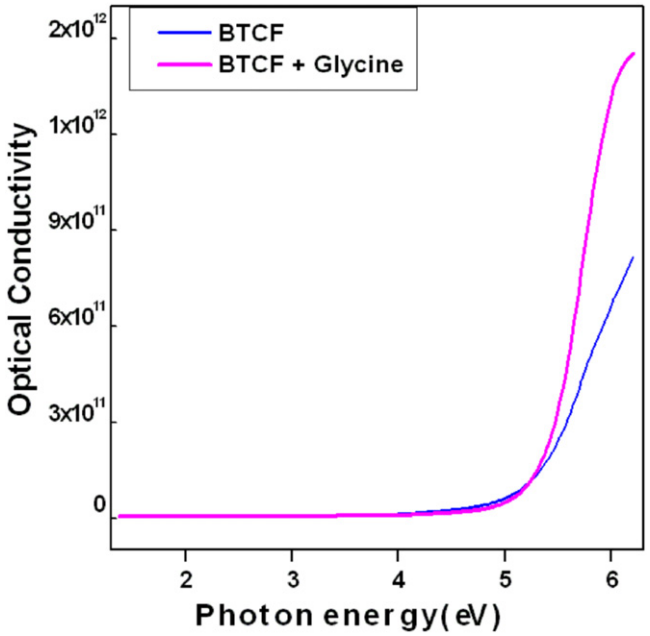

Figure 9. Plot of optical conductivity as a function of photon.

information processing and computing devices [16]. The doped BTCF crystal with promising optical properties emphasizes its prominence for distinct electro-optic applications.

3.4. Dielectric studies

The frequency (F) dependent dielectric studies of crystals were investigated at room temperature, using the Gwinstek-819 LCR meter. The relative permittivity of the material medium, i.e., the dielectric constant (ε_r), was determined using relation, $\varepsilon_r = Cd/\varepsilon_0 A$, where C is the capacitance of the sample, d is the thickness, ε_0 is the permittivity of free space, and A is the area of the sample crystal. The frequency response of the dielectric constant and dielectric loss of pure and doped BTCF crystals is shown in figures 10 and 11, respectively. The higher dielectric constant in the lower frequency region occurs due to active polarizations, namely, electronic, ionic, dipolar, and space charge, while disappearance of these polarizations leads to a lower dielectric constant at higher frequencies [20]. The comparatively lower dielectric constant of doped BTCF makes it a potential candidate for applications in microelectronics and electro optic modulator (EOM) devices [21]. The lower dielectric loss of

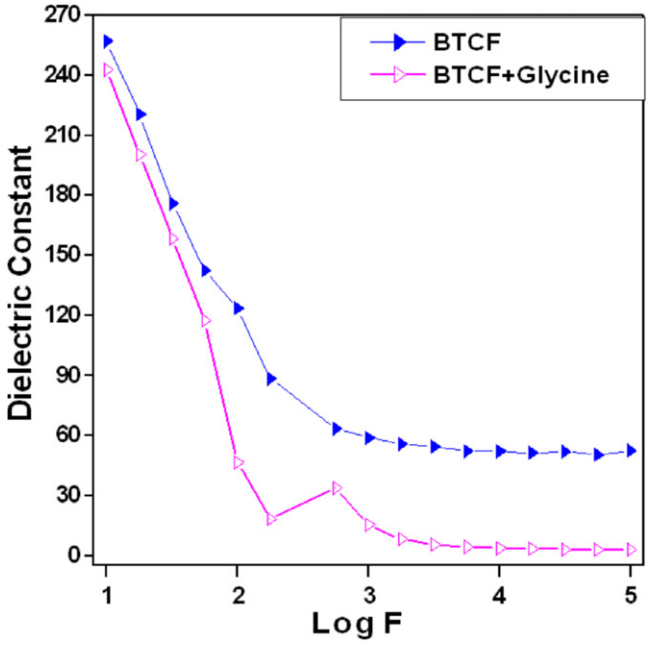

Figure 10. Frequency dependence of dielectric constant.

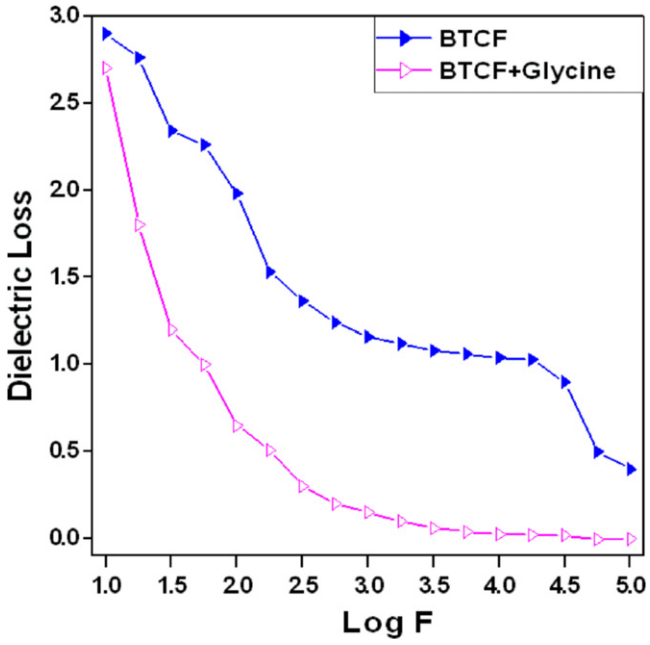

Figure 11. Frequency dependence of dielectric loss.

Table 2. Measurement details of Z-scan setup.

Laser beam wavelength (λ)	632.8 nm
Lens focal length (f)	12 cm
Optical path distance (Z)	115 cm
Spot-size diameter in front of the aperture (ω_a)	1 cm
Aperture radius (r_a)	4 mm
Incident intensity at the focus (Z = 0)	3.13 MW cm^{-2}

doped BTCF throughout the frequency range indicates the high optical quality and low energy dissipation when used as a dielectric medium [22]. The doping of glycine favored

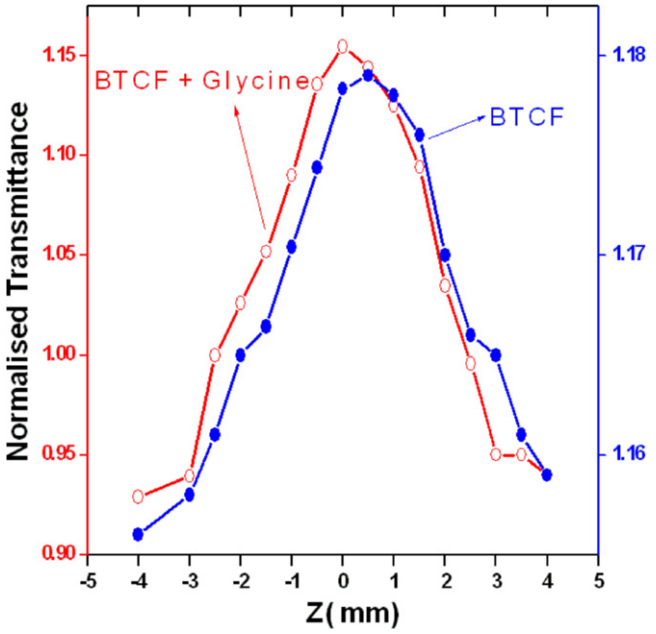

Figure 12. Open aperture normalized transmittance as a function of Z position.

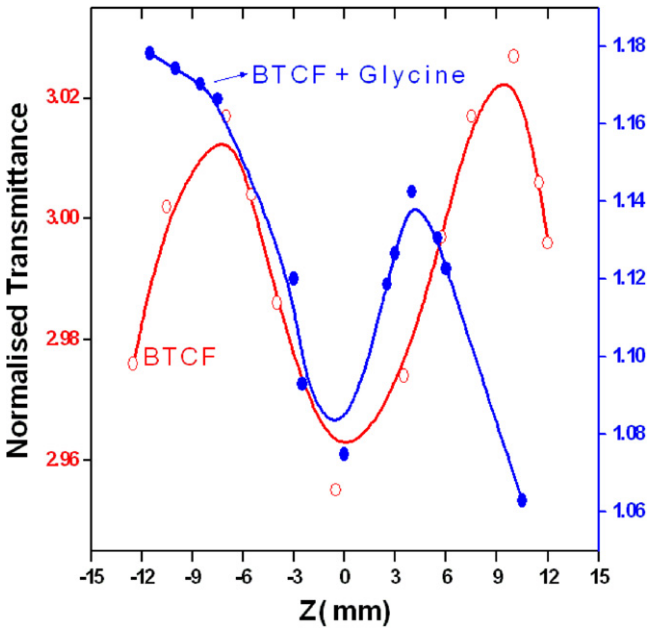

Figure 13. Closed aperture normalized transmittance as a function of Z position.

improved dielectric characteristics to BTCF, substantive for a high optical quality of crystal.

3.5. Third-order nonlinear optical studies

The Z-scan studies were performed to determine the third-order nonlinear response of pure and doped BTCF crystals. The well-polished, highly transparent 1 mm thickness samples of pure and doped BTCF crystals were used to collect the open and closed aperture transmittance data. The spectral

Table 3. Nonlinear optical parameters.

Sample	n_2 ($cm^2\ GW^{-1}$)	$\beta \times 10^{-9}$ ($cm\ W^{-1}$)	$\chi^3 \times 10^{-8}$ (*esu*)	FOM
BTCF	-9.04×10^{-4}	3.08	1.38	327
BTCF + glycine	1.01×10^{-5}	3.02	1.29	28 887

resolution of the Z-scan setup used in the present studies is detailed in table 2. The Gaussian beam of the Helium-Neon (He-Ne) laser operating at wavelength 632.8 nm was intended to focus on the sample through a convex lens of focal length 12 cm, and the sample was gradually translated along the Z direction. The peak to valley or valley to peak alterations in transmitted intensity along the focus (Z = 0) realizes the change in the refractive index of the crystal caused by localized absorption of the tightly focused optical field of the Gaussian beam [23].

The difference between the peak and valley transmission (ΔT_{p-v}) is calculated using equation [23],

$$\Delta T_{p-v} = 0.406(1 - S)^{0.25}|\Delta\phi|, \tag{3}$$

where $S = [1 - \exp(-2r_a^2/\omega_a^2)]$ is the aperture linear transmittance, r_a is the aperture radius, and ω_a is the beam radius at the aperture. The nonlinear refractive index (n_2) is calculated as [23],

$$n_2 = \frac{\Delta\phi}{KI_0L_{eff}}, \tag{4}$$

where $K = 2\pi/\lambda$ (λ is the laser wavelength), I_0 is the intensity of the laser beam at the focus (Z = 0), $L_{eff} = [1 - \exp(-\alpha L)]/\alpha$ is the effective thickness of the sample depending on linear absorption coefficient (α), and L is the thickness of the sample. The open aperture transmittance data of pure and doped BTCF evidences the saturable absorption depicted in figure 12. The nonlinear absorption coefficient (β) of both pure and doped BTCF can be evaluated using the open aperture transmittance data, according to the equation shown below [23],

$$\beta = \frac{2\sqrt{2}\Delta T}{I_0L_{eff}}, \tag{5}$$

where ΔT is the one valley value at the open aperture Z-scan curve. The third-order nonlinear susceptibility of the crystals was calculated using equations given by Bahae *et al* [23],

$$\mathrm{Re}\,\chi^{(3)}(esu) = 10^{-4}\left(\varepsilon_0 C^2 n_0^2 n_2\right)\Big/\pi\left(\mathrm{cm}^2/W\right) \tag{6}$$

$$\mathrm{Im}\,\chi^{(3)}(esu) = 10^{-2}\left(\varepsilon_0 C^2 n_0^2 \lambda\beta\right)\Big/4\pi^2(\mathrm{cm}/W) \tag{7}$$

$$\chi^3 = \sqrt{\left(\mathrm{Re}\,\chi^3\right)^2 + \left(\mathrm{Im}\,\chi^3\right)^2}, \tag{8}$$

where ε_0 is the vacuum permittivity, n_0 is the linear refractive index of the sample, and c is the velocity of light in vacuum. The pure BTCF crystal exhibits a self-defocusing nature, as the prefocal transmittance peak is followed by the postfocal transmittance valley, as depicted in figure 13. The self-defocusing nature of BTCF evidences the negative refraction nonlinearity, indicating its prominence for application in the protection of optical sensors in night vision devices [24]. The valley to peak transmittance configuration indicates the positive refraction nonlinearity of the glycine doped BTCF crystal, which is characteristic of material having a self-focusing tendency. The positive refraction nonlinearity of the doped BTCF crystal is a desirable property for the fabrication of optical switching devices [25]. The dopants with prominent π-bonding electrons have the tendency to alter the nonlinear refraction of the parent material, which is evident in the case of the glycine doped BTCF crystal [26]. The third order nonlinear susceptibility (χ^3) of the glycine doped BTCF crystal is 1.29×10^{-8} *esu*, which is greater than that of potassium dihydrogen phosphate (2.04×10^{-14} *esu*), lithium niobate (46.9×10^{-14} *esu*), and barium borate (2.4×10^{-14} *esu*) crystals [27]. The large nonlinear susceptibility of the material is manifested due to the active delocalization of the charge cloud of π-electrons in the molecular orbitals, formed by the superposition of intrinsic carbon P_z orbitals highly influenced by the incident optical field [28]. The higher figure of merit (FOM = $\beta\lambda/n_2$) of doped BTCF indicates the dominance of nonlinear refraction over the absorption coefficient, which is demanded for optical power limiting devices [29]. The comparative third-order nonlinear optical parameters of pure and doped BTCF are discussed in table 3.

4. Conclusion

The glycine doped BTCF crystal was successfully grown by a slow evaporation method. The observed shifts in the FT-IR spectrum confirmed the incorporation of glycine in the BTCF crystal. The glycine doped BTCF crystal with high optical transparency and a wider band gap of 5.16 eV is vital material for optoelectronics applications. The optical constants of BTCF were significantly improved due to the presence of glycine. The TGA curve of the doped BTCF crystal shows steady behavior up to 185 °C. The lower dielectric constant and dielectric loss of the glycine doped BTCF crystal are ideal parameters for microelectronics applications. The Z-scan study confirmed the effective third-order nonlinear behavior of pure and doped BTCF. The third-order nonlinear susceptibility of pure and doped BTCF crystals is higher than that of potassium dihydrogen phosphate, lithium borate, and barium borate crystals. The positive refraction nonlinearity of the doped BTCF crystal suggests its prominence for optical switching and optical limiting devices.

Acknowledgments

The authors are grateful to the Department of Science and Technology (DST/SR/S2/LOP-22/2010) and University Grants Commission (UGC/41-591/2012/SR), New Delhi, for financial assistance. The authors are also grateful to Prof. Sastikumar, Department of Physics, NIT, Tirucherappalli, for extending the Z-scan facility.

References

[1] Quasim I, Firdous A, Khosa S K and Kotru P N 2009 *J. Phys. D: Appl. Phys.* **42** 155505
[2] Bouchouit K, Kouissa B, Migalska-Zalas A, Brihi N and Sahraoui B 2013 *Opt. Quant. Electron.* **46** 111–6
[3] Helina B, Selvarajan P and Lucia Rose A S J 2012 *Phys. Scr.* **85** 055803
[4] Selvakumar S, Ravi Kumar S M, Rajarajan K, Joseph Arul Pragasam A, Rajasekar S A, Thamizharasan K and Sagayaraj P 2006 *Cryst. Growth Des.* **6** 2607
[5] Shahil Kirupavathy S, Stella Mary S, Srinivasan P, Vijayan N, Bhagavannarayana G and Gopalakrishnan R 2007 *J. Cryst. Growth* **306** 102
[6] Rajasekaran R, Ushasree P M, Jayavel R and Ramasamy P 2001 *J. Cryst. Growth* **229** 563
[7] Moitra S, Bhattacharya S, Kar T and Ghosh A 2008 *Phys.* B **403** 3244
[8] Anie Roshan S, Cyriac J and Ittyachen M A 2001 *Mater. Lett.* **49** 299
[9] Selvaraju K, Valluvan R and Kumararaman S 2006 *Mater. Lett.* **60** 3130
[10] Selvaraju K, Valluvan R and Kumararaman S 2007 *Mater. Lett.* **61** 751
[11] Ravi Kumar S M, Melikechi N, Selvakumar S and Sagayaraj P 2008 *Phys.* B **403** 4160
[12] Dhumane N R, Hussaini S S, Dongre V G and Shirsat M D 2008 *Opt. Mater.* **31** 328
[13] Dhumane N R, Hussaini S S, Dongre V G, Karmuse P P and Shirsat M D 2009 *Cryst. Res. Technol.* **44** 269
[14] Hussaini S S, Dhumane N R, Dongre V G and Shirsat M D 2008 *Opt. Advnc. Mater.* **2** 108
[15] Prasanyaa T, Haris M, Jayaramakrishnan V, Amgalan M and Mathivanan V 2013 *Phys. Scr.* **88** 045403
[16] Shaikh R N, Mohd A, Gambhire A B, Shirsat M D and Hussaini S S 2014 *Mater. Res. Express* **1** 015016
[17] Mohd A, Shaikh R N, Shirsat M D and Hussaini S S 2014 *Opt. Laser Technol.* **60** 124
[18] Kalaiselvi D and Jayavel R 2012 *Appl. Phys.* B **107** 93
[19] Sabari Girisun T C and Dhanuskodi S 2009 *Cryst. Res. Technol.* **44** 1297
[20] Dhanaraj P V and Rajesh N P 2011 *J. Cryst. Growth* **318** 974
[21] Shanmugam G, Thirupugalmani K, Rakhikrishna K, Philip J and Brahadeeswaran S 2013 *J. Therm. Anal. Calorim.* **114** 1245–54
[22] Soma A and Tanusree K 2012 *Mater. Chem. Phys.* **133** 1055
[23] Bahae M S, Said A A, Wei T H, Hagan D J and Van Stryland E W 1990 *IEEE J. Quant. Electron.* **26** 760
[24] Subhashini V, Ponnusamy S and Muthamizhchelvan C 2013 *J. Cryst. Growth* **363** 211
[25] Ashok Kumar R, Ezhil Vizhi R, Vijayan N, Bhagavannarayana G and Rajan Babu D 2010 *J. Pure Appl. & Ind. Phys.* **1** 61
[26] Mohd A, Shirsat M D, Muley G and Hussaini S S 2014 *Phys.* B **449** 61
[27] Srinivasan P, Nooraldeen A Y, Kanagasekaran T, Dhinaa A N, Palanisamy P K and Gopalakrishnan R 2008 *Laser Phys.* **18** 790
[28] Singh V, Aghamkar P and Malik R K 2013 *Appl. Phys.* B **115** 391–9
[29] Kanagasekaran T, Mythili P, Srinivasan P, Nooraldeen A Y, Palanisamy P K and Gopalakrishnan R 2008 *Cryst. Growth Des.* **8** 2335